

https://doi.org/10.1070/QEL17275

Experimental investigation of laser ablation of stone polycrystalline targets

I.N. Burdonskii, A.G. Leonov, K.N. Makarov, V.N. Yufa

Abstract. **We report the results of an experimental investigation of ablation of stone polycrystalline targets of complex multicomponent composition, which imitate the substance of asteroids. The targets were irradiated by nanosecond pulses of a neodymium laser at an energy density Φ_L of up to 5×10^4 J cm^{-2}. The experiments demonstrated the existence of two ablation regimes, with the boundary between them lying at $\Phi_L \approx 4000$ J cm^{-2}. The regime change is characterised by a change in the form of the dependence of the surface mass density of removed target material on the laser energy density and by the appearance of a minimum in the dependence of specific energy of destruction on Φ_L. This is supposedly related to the passage from a one-dimensional plasma plume expansion to the three-dimensional one and the corresponding decrease in the efficiency of energy transfer from the laser beam to the target due to a lowering of laser-produced plasma density. Our experiments also showed the existence of a maximum in impulse coupling coefficient C_m as a function of laser energy density ($C_m \approx 6.3\times10^{-5}$ N W^{-1} for $\Phi_L = \Phi_{opt} \approx 25$ J cm^{-2}). Maxima were also recorded in the dependences of the ablation efficiency and average ablation flow velocity on Φ_L. For $\Phi_L > \Phi_{opt}$, the decrease in the function $C_m(\Phi_L)$ turns out to be much steeper than for metals and polymer materials. The difference is supposedly due to the lower strength and lower plasticity of the polycrystalline stone targets.**

Keywords: *laser ablation, plasma plume, stone targets, impulse coupling coefficient, asteroid deflection.*

1. Introduction

Due to the remarkable progress in the development of high-power lasers, the last decade has seen a growing interest towards the use of laser ablation as a source of jet thrust for the contactless deflection of massive objects (primarily, asteroids) from their orbits that pass in the dangerous vicinity of the Earth. Different approaches are introduced for the solution of this problem: destruction by a nuclear explosion, the impact of a kinetic projectile, gravity towing, etc. [1]. However, as shown in Refs [2, 3], one of the most efficient means of action is the ablation of the asteroid surface layers under high-power laser irradiation. In this case, the evaporated substance forms a high-intensity jet, which generates a recoil momentum and deflects the object from the potentially dangerous trajectory. References [2, 3] also provide estimates of the radiation power, irradiation time, and other interaction parameters, which show the feasibility of laser-based deflection techniques.

The most important parameter defining the ablation efficiency is the impulse coupling coefficient C_m, which appears under high-power irradiation. It is defined as the ratio between the mechanical momentum $M_t\delta V_t$ acquired by the target (M_t is the target mass and δV_t is the velocity increment due to the recoil momentum) and the energy E_L of a laser pulse (for a pulsed irradiation regime):

$$C_m = M_t\delta V_t/E_L = \delta M_t V_e/E_L = \mu V_e/\Phi_L, \quad (1)$$

where δM_t is the target mass loss arising from the laser ablation; μ is the mass loss per unit irradiation area; V_e is the average velocity of the ablation jet; and Φ_L is the energy density in the target irradiation zone. It is common knowledge (see, for instance, work [4] and references therein) that the impulse coupling coefficient C_m as a function of Φ_L (or of the radiation intensity I_L) increases steeply on exceeding the ablation threshold, reaches its maximum, and then begins to decrease with increasing Φ_L. In this case, $C_m \propto \Phi_L^{-n}$, where the exponent n, as a rule, lies in the range ~0.2–0.4, depending on the interaction parameters.

Other important characteristics of laser ablation that define its efficiency and recoil momentum are the ablation efficiency and the mass of substance ejected from the crater in relation to the energy parameters of the laser beam incident on the target surface. In our work, the term ablation efficiency η is used in reference (following Refs [4, 5]) to the ratio of the kinetic energy E_k of ablation jet to the energy of the laser pulse:

$$\eta = E_k/E_L = \psi\delta M_t V_e^2/(2E_L) = \psi C_m V_e/2, \quad (2)$$

where $\psi = \langle V_x^2\rangle/\langle V_x\rangle^2$ and V_x is the velocity component of ablation jet particles perpendicular to the target surface. The introduction of the parameter ψ describes the fact that the particle velocity distribution in the ablation jet is Maxwellian with a nonzero average drift velocity $V_e \equiv \langle V_x\rangle$ [5, 6]. As shown in these works, the parameter ψ does not differ significantly from unity when the laser intensity is sufficiently high. To reliably predict the results of action on asteroids and develop a scenario for this action, it is necessary to have reliable data

I.N. Burdonskii, K.N. Makarov, V.N. Yufa State Research Centre of Russian Federation 'Troitsk Institute for Innovation and Fusion Research', ul. Pushkovykh, vlad. 12, 108840 Moscow, Troitsk, Russia; Moscow Institute of Physics and Technology (National Research University), Institutskii per. 9, 141701 Dolgoprudnyi, Moscow region, Russia;
A.G. Leonov Moscow Institute of Physics and Technology (National Research University), Institutskii per. 9, 141701 Dolgoprudnyi, Moscow region, Russia; e-mail: leonov@phystech.edu

Received 22 October 2010
Kvantovaya Elektronika **50** (8) 763–769 (2020)
Translated by E.N. Ragozin

describing the dependence of C_m and η values on different parameters (irradiation energy, characteristics of the substance of a dangerous object, etc.) that can be obtained in model experiments. In fact, it is necessary to estimate the radiation energy density at which η and C_m reach their maximum, the C_m maximum itself, as well as the exponent n.

The dependences of C_m on the energy of laser radiation incident on the surface of a metal or polymer surface were investigated in many papers, particularly in the feasibility studies of propulsors harnessing laser-driven jet thrust (see, for instance, Refs [4, 7–12]). However, the data on the specific mechanical momentum produced in the irradiation of stone polycrystalline targets of complex composition (whose thermophysical and optical properties are radically different from those of metals, semiconductors and transparent dielectrics, including polymers) are, to the best of our knowledge, absent in the literature. It is pertinent to note that precisely the stone (chondrite) asteroids account for ~90% of all asteroids. Furthermore, the investigation of laser radiation interaction with relatively weakly absorbing polycrystalline multicomponent targets, including ceramics, mountain rock, etc., are also of considerable interest from the standpoint of potential technological applications.

To bridge this gap, in this paper we present the results of experimental investigations to determine the laser ablation characteristics for stone targets of various types that imitate the substance of asteroids. This opens up the possibility to employ laser radiation for deflecting dangerous cosmic objects due to the recoil momentum arising from the evaporation of their surface layers.

2. Experimental facility and diagnostic methods

Our investigations were carried out on a 'Saturn' laser facility [13, 14]. It comprises a high-power multistage phosphate Nd^{3+}-glass laser with an automated system for active medium pumping, a vacuum interaction chamber, and a diagnostic complex. The laser parameters are as follows: energy $E_L \leqslant 50$ J, wavelength $\lambda = 1.054$ μm, pulse duration $\tau_L = 30$ ns (FWHM), and divergence $\theta \approx 1.5\times10^{-4}$ rad.

In the experiments performed to measure the recoil momentum, use was made of the variously shaped artificial chondrite targets placed at our disposal by the Russian Federal Nuclear Centre–All-Russian Scientific Research Institute of Experimental Physics (RFNC-VNIIEF), as well of targets made of natural andesite (volcanic mountain rock, whose composition is similar to the composition of the substance of some meteorites and individual Martian rocks [15, 16]). Furthermore, also investigated in several experiments was the ablation of a target made of the fragments of the Chinge iron meteorite [17], which contains iron (82.8%), nickel (16.6%), cobalt (0.55%), phosphorus (0.05%), as well as trace impurities of Ga, Ge, and Ir. Here and below the content of a substance is given in mass percent.

The artificial targets were made with the technology described at length in Ref. [18]. The chemical composition of these targets (40% SiO_2, 26% MgO, 18% Fe_2O_3, 6% FeS) corresponded approximately to that of the 'Chelyabinsk' meteorite, which belongs to the class of ordinary chondrites; the target densities were ~2.3 g cm^{-3}. For comparison, we used in experiments the targets with different compressive strength $\sigma = 27$ and 134 MPa.

Like chondrites, andesite is characterised by a large fraction of silica SiO_2, whose content amounts to 52% – 65%. However, unlike chondrites, andesites contain a rather large fraction of Al_2O_3 (~17%) and a considerably lower amount of MgO (~3%) [19]. Andesite also contains the oxides of other light elements: CaO, Na_2O, K_2O. The content of the oxides of heavier elements (P_2O_5, Fe_2O_3, FeO, TiO_2, MnO) in andesite is exactly ~8%. The measured density of andesite samples $\rho \approx 2.4 \pm 0.1$ g cm^{-3}, which corresponds to the figures given in Ref. [19]. Special measurements of their strength were not performed in our work. However, it is well known that the compressive strength of andesite may be as high as 240 MPa [19].

In our experiments we investigated targets of mass 0.05–0.3 g with a characteristic size of 3.5–5 mm. Prior to placing the target into the interaction chamber, the surface to be irradiated was ground and polished. The laser focal spot diameter d (by the $1/e^2$ level) was varied in the range 0.3–3.5 mm by displacing the focusing objective lens, which permitted performing velocity measurements at intensities of up to 2×10^{12} W cm^{-2}.

The recoil momentum produced by laser ablation was recorded by the ballistic pendulum method. To this end, the targets were suspended on thin fibres behind the focal plane of the input lens in the vacuum interaction chamber (the residual gas pressure in the chamber did not exceed 10^{-3} mm Hg). To determine the impulse coupling coefficient in experiments, the initial velocity of the target of known mass, which was acquired under laser irradiation, was measured in two independent ways. This approach makes it possible to determine the total mechanical momentum imparted to the target without the necessity of including the friction loss and several other uncertainties.

In the former case, the target velocity was measured with a photon Doppler velocity (PDV) metre designed and made in the National Research Nuclear University MEPhI (for more details, see Refs [20, 21]). This measurement technique relies on the recording of the Doppler-shifted component of the radiation of a single-frequency cw laser and mixing the probing wave reflected from the object with the unperturbed reference wave. For this purpose, behind the target in the direction of the beam we placed a collimator with a wide-angle microlens ('g-lens') coupled to the analyser by a fibre line. The target surface had a low reflection coefficient, and so an ~0.1-μm thick aluminium layer was deposited on the rear surface of the target to improve the sensitivity of the PDV diagnostics.

The beat frequency is related to the target velocity by the formula $f = \delta V_t/\lambda$, where $\lambda = 1.55$ μm is the probing radiation wavelength. The beat recording time was of the order of tens and hundreds of microseconds, which made it possible to measure the target velocity with an uncertainty below 5%–10% even when measuring low velocities (~0.1 m^{-1}).

The latter technique relied on the use of a time-of-flight scheme and the photographic recording of the target motion (illuminated by semiconductor laser radiation in the green region of the spectrum) with a Canon G15 camera operated at a frequency of 240 frames per second. The camera triggering was timed to the onset of a laser pulse. The target velocity was determined by measuring the length of its image track in an individual frame or the target displacement in several sequential frames for low recoil momenta. In both cases, the uncertainty of velocity measurements did not exceed 5%–10%. We note that the data obtained with the PDV metre and the fast photographic camera were consistent to within the same uncertainty (~10%), which bears out the accuracy of measurements.

In addition to impulse coupling coefficient measurements, we measured the mass removal under laser irradiation. The

mass removal was determined by weighing the target with analytical weights prior to and after laser irradiation with an accuracy of $\sim 10^{-5}$ g and checked by measuring the volume of the crater produced on the target surface. The crater's shape and parameters were recorded by optical methods (with an MML-3 metallographic microscope) as well as by the mechanical profilometers Mitutoyo Surftest (SJ-210 series) and Dektak 150. The uncertainties of crater's depth and diameter measurements were 1 and 10 μm, respectively. The mass removal data determined by target weighing and those calculated proceeding from the crater volume measurements coincided to within 20%–30%. For low mass removals (under 3×10^{-5} g), the mass was determined only from the crater volume.

3. Measurement results and their discussion

As noted above, one of the most significant characteristics of laser ablation is the dependence of the mass of substance ejected from the crater on the energy of a laser pulse. Figures 1 and 2 depict the measurement data for the surface mass density μ of removed target substance (the target mass removal divided by the area of irradiated surface) in relation to the laser beam energy density Φ_L in the range $50-5\times10^4$ J cm^{-2} for the targets of different strength and for different focal spot diameters d. It is noteworthy that all measurements of the present work were performed for irradiation intensities I_L by far greater than the breakdown thresholds for the vapour of target substance in vacuum. It is well known (see, for instance, Refs [22, 23]) that the typical breakdown threshold intensities for dielectrics in the nanosecond pulse duration range are about 10^9 W cm^{-2} (for conducting materials it may be lower by an order of magnitude), which corresponds to a laser beam energy density of only 30 J cm^{-2} under our conditions. Therefore, all our experiments were carried out in the hydrodynamic irradiation mode, which consists in the production of a laser-produced plume and the transfer of absorbed laser energy to the target substance with the prevalent role of hydrodynamic energy transfer mechanism [13, 22, 24, 25].

Experimental data demonstrate that a three-fold variation of the spot size d, from 0.035 to 1 mm (Fig. 1), hardly affects, to within the spread of the experimental data, the dependences $\mu(\Phi_L)$. The data for andesite and artificial chondrites of different strength (27 and 134 MPa) also agree nicely with each other within the limits of experimental error (Fig. 2), i.e. the material strength, as would be expected, is not a significant factor determining the ablation of the targets exposed to high-power laser radiation at an intensity of 10^9-10^{12} W cm^{-2}. A small discrepancy in the values of mass removal for chondrite samples of different strength at $\Phi_L > 10^4$ J cm^{-2} can be explained by the occurrence of experimentally observed crushing followed by the shedding of some target surface layers with a strength of 27 MPa under the action of a shock wave produced by the pressure pulse of the laser-vaporised substance.

From the data presented in Figs 1 and 2 it follows than an appreciable mass removal ($\mu > 0.1$ mg cm^{-2}) begins for a laser energy density of the order of several tens of J cm^{-2}, and the μ value grows almost linearly with Φ_L. The least-squares best fit to data points of the entire collection of experimental data, which were obtained in experiments on chondrite targets for different focal spot dimensions and different strengths, shows that, in the range 50–4000 J cm^{-2}, $\mu \propto \Phi_L^{\beta}$ with the exponent $\beta \approx 1.2$. The approximative curve for the andesite target is hardly different from the corresponding curve for the chondrite targets and is therefore not shown in Fig. 2.

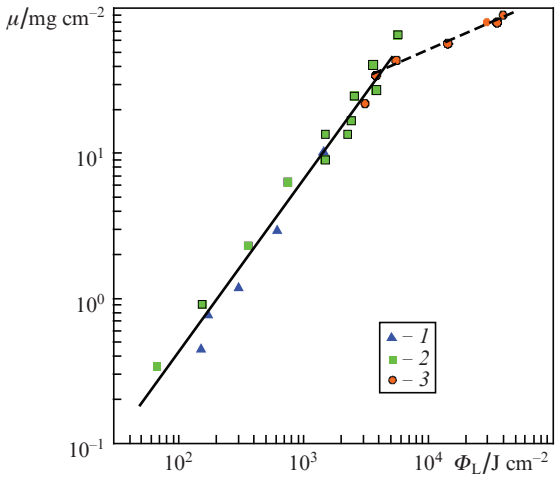

Figure 1. (Colour online) Surface mass density μ of removed target material as a function of laser energy density Φ_L for a focal spot size d = (*1*) 0.1, (*2*) 0.075, and (*3*) 0.035 cm for a chondrite target of strength σ = 27 MPa. The solid line approximates the experimental data in the range 50–4000 J cm^{-2} ($\mu \propto \Phi_L^{1.2}$) and the dashed line in the domain $\Phi_L > 4000$ J cm^{-2} ($\mu \propto \Phi_L^{0.4}$).

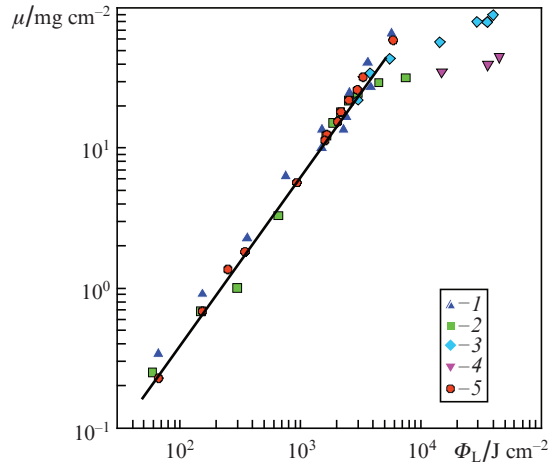

Figure 2. (Colour online) Surface mass density μ of removed target material as a function of laser energy density Φ_L for artificial chondrites of different strength (*1*–*4*) and for andesite (*5*) for (*1*) d = 0.075 cm, σ = 27 MPa; (*2*) d = 0.075 cm, σ = 134 MPa; (*3*) d = 0.035 cm, σ = 27 MPa; (*4*) d = 0.035 cm, σ = 134 MPa; and (*5*) d = 0.075 cm. The solid line approximates the entire collection of experimental data obtained for chondrite targets in the range 50–4000 J cm^{-2} ($\mu \propto \Phi_L^{1.2}$).

We note that there is no way of determining the targets ablation thresholds by extrapolating the resultant data to the zero values of mass removal in the experiments under consideration: as is well known (see, for instance, Refs [23, 26, 27]), the $\mu(\Phi_L)$ dependence for low energy densities of the laser beam is strongly nonlinear and calls for additional investigations. However, in this work we did not set ourselves the task of measuring the thresholds, because, considering the structural inhomogeneity of polycrystalline targets, the mass removal in this interaction parameter domain may be correctly determined only under multiple target irradiation in a laser pulse repetition regime due to a low mass removal and small crater depths produced under single-pulse irradiation.

When the laser energy density becomes higher than ~4000 J cm^{-2}, the $\mu(\Phi_L)$ dependence moderates its growth rather sharply, and approximating the data in this domain results in the dependence $\mu \propto \Phi_L^{0.4}$ (see Fig. 1).

The experimental data on mass removal found in the literature apply mostly to metal targets and relatively low Φ_L values: below 100–500 J cm^{-2} [23]. However, the characteristic values of μ in this domain are close to those measured in the present work. As noted in Ref. [23], the ablation intensity is determined by a complex combination of optical, thermophysical, and strength material properties, with the result that the surface mass densities of removed target material for the same radiation energy density at the target surface may be close for materials with strongly different properties. For instance, for several metals (Al, Ti, Cu) $\mu \approx 1.5$–3.5 mg cm^{-2} for a radiation energy density of ~500 J cm^{-2} ($\lambda = 1.06$ μm) in the nanosecond range of laser pulse duration [23]. In our experiments, $\mu \approx 3$ mg cm^{-2} for the same Φ_L value. For graphite, $\mu \approx 0.7$ mg cm^{-2} for $\Phi_L \approx 50$–100 J cm^{-2} [27, 28] (in the present work, $\mu \approx 0.4$ mg cm^{-2} for $\Phi_L = 100$ J cm^{-2}).

The energy density domain $\Phi_L \approx 5\times10^2 - 10^5$ J cm^{-2} has been significantly less investigated. We mention only the experimental results obtained using the PALS iodine laser radiation ($\lambda = 1.315$ μm) for a pulse duration of 0.3–0.4 ns [29, 30]. As determined, in particular, in these works, for an energy density of the order of 10^4–10^5 J cm^{-2}, the mass removal in the irradiation of aluminium and tantalum targets was ~30–200 mg cm^{-2}, which is only one-and-a-half to two times different from the μ values determined for similar Φ_L values in our work.

Figure 3 shows the effective specific energy of target material disruption (the energy of a laser pulse divided by the mass of removed material) as a function of Φ_L for different irradiation spot diameters and chondrite targets of different strength. Referring to Fig. 3, with increasing the radiation energy density in the range $\Phi_L \approx 50$–4000 J cm^{-2} the specific disruption energy initially becomes somewhat lower (approximately by a factor of two-to-three with increasing Φ_L by two orders of magnitude) and then begins to increase rapidly. The minimum of $\varepsilon(\Phi_L)$ is approximately in the same domain ($\Phi_L \approx 4000$ J cm^{-2}) in which the slope of the $\mu(\Phi_L)$ dependences changes.

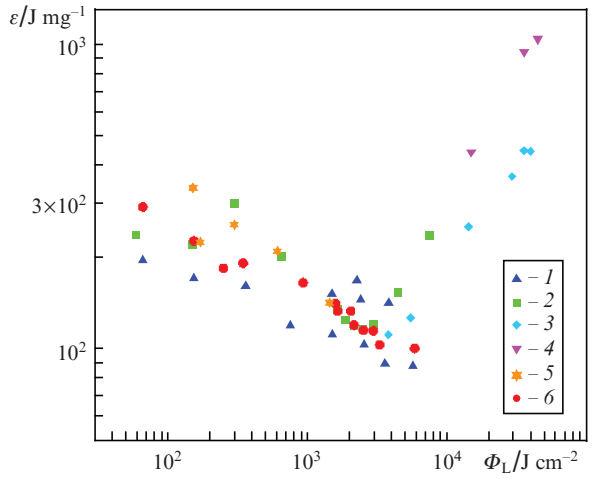

Figure 3. (Colour online) Dependences of the effective specific disruption energy on the laser energy density for artificial chondrites of different strength (*1*–*5*) and andesite (*6*) for (*1*) $d = 0.075$ cm, $\sigma = 27$ MPa; (*2*) $d = 0.075$ cm, $\sigma = 134$ MPa; (*3*) $d = 0.035$ cm, $\sigma = 27$ MPa; (*4*) $d = 0.035$ cm, $\sigma = 134$ MPa; (*5*) $d = 0.1$ cm, $\sigma = 27$ MPa; and (*6*) $d = 0.075$ cm.

In this case, the laser energy expenditures for the removal of a unit target mass (10^2 – 10^3 kJ g^{-1}, see Fig. 3) turn out to be significantly higher than the sublimation energy Q of the same amount of ejected target material throughout the Φ_L energy range investigated. According to Ref. [31], for silicon dioxide SiO_2, which is the main constituent of andesite [19] as well as of model chondrite targets [18], the energy $Q = 9.75$ kJ g^{-1} (we note that a figure of 5 kJ g^{-1} was assumed as the average Q value in the calculation of asteroid characteristics in Ref. [32]). Therefore, a significant fraction of the laser energy is expended for the absorption in the laser plume and increases the thermal and kinetic energy of the vaporised target material.

In this connection it is pertinent to note that the stationary evaporation regime [24] cannot be the cause of the close-to-linear growth of the function $\mu(\Phi_L)$ for $\Phi_L < 4000$ J cm^{-2}. The special feature of stone targets is that their absorption coefficients for laser radiation are rather small in comparison, for example, with those for metals. In this case, the absorption depth turns out to be much longer than the characteristic distance through which heat propagates during the course of a laser pulse, $D \approx (\chi\tau_L)^{1/2}$, where χ is the thermal diffusivity. Therefore, we are dealing with a volume character of absorption and the target material heating due to the thermal conductivity beyond the absorption zone is insignificant. For instance, for andesite $\chi = 6.3\times10^{-3}$ cm^2 s^{-1} [33] and $D \approx 1.4\times10^{-5}$ cm for $\tau_L = 30$ ns. The absorption coefficient α of mountain rock at $\lambda = 1.05$ μm lies between 10 and 100 cm^{-1} [13, 34] and therefore the absorption depth may range up to tenths of a millimetre.

In the case of surface absorbers (metals), $\alpha \approx 10^5$ cm^{-1}, $\chi \approx 0.1 - 1$ cm^2 s^{-1} and $\alpha D \gg 1$. For these parameters, the stationary evaporation regime is, as a rule, reached even at relatively low intensities, which are below the threshold of surface plasma production [24]. As shown in Ref. [23], in the case of metals a linear dependence $\mu(\Phi_L)$ is indeed observed for nanosecond pulses up to an energy density of ~50 J cm^{-2}, as long as the absorption in the plasma plume may be thought of as being insignificant. For a volume absorber (andesite), the time of reaching the stationary evaporation regime $t_{st} \propto (1/\alpha)\times(Q\rho/I_L)$ is comparable with the laser pulse duration for $I_L \approx 10^{10} - 10^{11}$ W cm^{-2} (depending on the α magnitude). However, in this domain the practically total absorption of laser radiation in the plasma plume radically changes the kinetics of the disruption of target surface layers, which now is determined by the hydrodynamic energy transfer from the radiation to the surface. The efficiency of conversion of the laser energy absorbed in the plasma to the energy of the shock wave propagating in the solid part of the target is low [25, 29], which accounts for high specific disruption energy (for andesite, as estimated in Ref. [13], the conversion efficiency is 2% – 5% in the intensity range $I_L \approx 10^{11} - 10^{12}$ W cm^{-2}). Moreover, the hydrodynamic ablation mechanism depends only slightly on the material properties and, in particular, on how high is the absorption coefficient for laser radiation in the target material, which may account for the close values of mass removal for minerals and metals. The occurrence of a strong shock wave is also attributed to the fact that the crater size in andesite samples for a small diameter of the laser beam is significantly greater than the size of the focal spot on the target surface [13].

Generally speaking, a theoretical description of the ablation of a target of complex composition with the inclusion of its screening by surface laser-produced plasma calls for cumbersome numerical simulations. In the hydrodynamic regime, however, some important results may be obtained even from simple physical considerations by invoking conservation laws and assuming the quasi-stationarity of ablation plasma flow. In Ref. [35] (see also Ref. [22]) an analysis was performed of the theoretical scalings calculated in several papers, which showed that the exponent β varies, depending on the calculation details, in the range 0.33–0.56, which agrees, by and large, with the $\mu(\Phi_L)$ dependence measured in our work for a high radiation energy density.

It is noteworthy that the experimentally determined $\varepsilon(\Phi_L)$ dependence is in qualitative agreement with the theoretical notions developed in Ref. [29]. According to these notions, in the hydrodynamic regime the mass removal is determined by the properties of the laser plume, in which the energy of a laser pulse is converted to the energy of a shock wave, which results in the disruption of the target surface. In this case, the relative energy expenditures for the target material disruption decrease with increasing radiation intensity because of absorption growth in the plasma plume under the conditions of prevalence of the inverse bremsstrahlung and, accordingly, enhancement of the energy transfer efficiency from the laser beam to the target. On the other hand, at some intensity the energy transfer efficiency begins to decrease due to the density lowering of the laser-produced plasma in going from the one-dimensional plasma plume expansion to the three-dimensional expansion regime (for more details, see Ref. [29]). This results in the growth of specific energy of target disruption and accounts for the appearance of the minimum in the $\varepsilon(\Phi_L)$ dependence. Specifically, according to the measurements and simulations of Ref. [14], for $\Phi_L \approx 4000$ J cm^{-2} the plasma plume temperature at the andesite target is 150 eV and the plasma sound velocity V_s amounts to $\sim 5\times10^6$ cm s^{-1}. If it is assumed that the plasma expansion velocity is close to the sound velocity, during the course of the laser pulse the plasma will have time to expand to a distance of the order of the doubled focal spot size for $d = 0.075$ cm.

Figure 4 shows the dependences of impulse coupling coefficient C_m on the energy density of laser pulses for chondrite targets of strength 27 and 134 Pa, which were constructed from the initial velocity measurements for a ballistic pendulum of known mass. With reference to Fig. 4, for low Φ_L values the impulse coupling coefficient rapidly increases with radiation energy density and reaches its maximum ($C_m \approx 6.3\times 10^{-5}$ N W^{-1}) for the optimal value $\Phi_L = \Phi_{opt} \approx 25$ J cm^{-2}. Further increase in Φ_L results in a monotonic lowering of C_m. As mentioned in the foregoing, this behaviour of the $C_m(\Phi_L)$ dependence has been repeatedly observed for metals and polymer materials (see, for instance, Refs [4, 7, 36, 37]). However, for these materials, the optimum was observed at Φ_L values that were several times lower than those measured for stone targets in this paper. Note that, based on the analysis of numerous data, in Ref. [4] it was shown that the position of the maximum is close to the plasma production threshold in a broad range of radiation wavelength and pulse duration and is nicely described by the empirical dependence $\Phi_{opt} \approx 4.8\times10^4\ \tau_L^{1/2}$ (Φ_{opt} is measured in J cm^{-2} and τ_L in seconds), which gives a figure of 8.3 J cm^{-2} for the conditions of our work.

In the laser energy density region $\Phi_L > \Phi_{opt}$, approximating the resultant data by the best-fit trend line shows that C_m

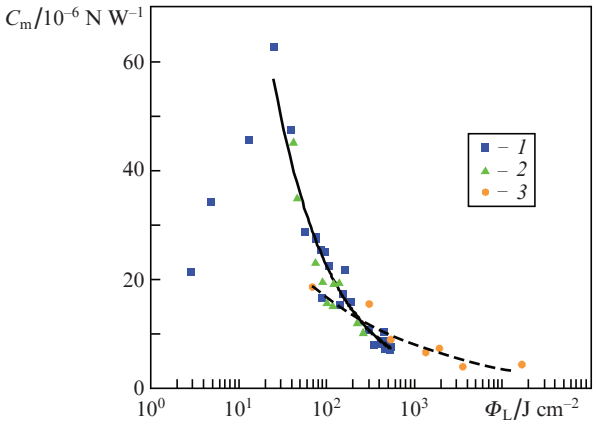

Figure 4. (Colour online) Dependences of impulse coupling coefficient on the laser energy density for chondrite targets with a strength $\sigma = (1)$ 27 and (2) 134 MPa as well as (3) for the iron-nickel target (a fragment of the Chinge meteorite). The solid line approximates the collection of experimental data for chondrite targets in the domain $\Phi_L > 25$ J cm^{-2} ($C_m \propto \Phi_L^{-0.66}$) and the dashed line approximates the data for the iron-nickel target ($C_m \propto \Phi_L^{-0.3}$).

$\propto \Phi_L^{-n}$ with the exponent $n = 0.66$. This n value is significantly different from the exponent that characterises the more gently sloping dependences $C_m(\Phi_L)$ obtained experimentally for metals and polymer materials ($n \approx 0.3$). As shown in Ref. [7], above the breakdown threshold the simplified stationary analytical model of the laser-produced plasma plume, which implies that the inverse bremsstrahlung is the main mechanism of laser radiation absorption and which adequately describes experimental data in a broad parameter domain, predicts the dependence of impulse coupling coefficient on the radiation energy density of the form $C_m \propto \Phi_L^{-0.25}$. To compare the characteristics of the action on stone and metal targets, we measured the impulse coupling coefficient in the irradiation of the target made of a fragment of the iron-nickel Chinge meteorite (Fig. 4). Our experiments suggest that the experimental data in this case are nicely approximated by the dependence $C_m \propto \Phi_L^{-n}$ with the exponent $n = 0.3$, i.e. are quite consistent with the experimental data obtained for metals in other works.

The set of measurements of the mass removal μ and impulse coupling coefficient C_m permitted us to construct the dependence of ablation efficiency η [see formula (2)] on the energy density Φ_L. In view of formula (1), we rewrite expression (2) in the form ($\psi \approx 1$):

$$\eta = C_m V_e/2 = C_m^2\, \Phi_L/(2\mu). \qquad (3)$$

Since the quantities μ and C_m were measured in independent experiments, to determine η in the range $\Phi_L < 4000$ J cm^{-2} we used the $\mu(\Phi_L)$ approximation of the form $\mu(\Phi_L) = 1.73\times10^{-3}\Phi_L^{1.2}$. The $\eta(\Phi_L)$ dependence obtained in this way for the irradiation of chondrite targets with a density of 27 MPa is depicted in Fig. 5. One can see that the ablation efficiency, like C_m, peaks for Φ_{opt} and amounts to 0.6. Figure 5 also shows the Φ_L dependence of the average particle velocity $V_e = C_m\Phi_L/\mu$ in the ablation jet calculated using the same approximation for μ. This dependence shows a somewhat unexpected result: V_e decreases in magnitude with increasing energy density Φ_L. It is believed that this dependence is due to a large fraction of the melt droplets of the target material in the ablation stream. In the earlier investigations of andesite

ablation for close interaction parameters [13], a scanning electron microscope study of the composition of the film deposited on a silicon substrate by the laser-produced plume showed that a large amount of solidified micrometre-sized droplets does exist in the substance ejected from the crater. The velocity V_e is in fact found from the momentum conservation law and is the velocity averaged over all components of the ablation stream. Similarly, the ablation efficiency is determined via the averaged velocity V_e. In reality, there are, roughly speaking, two components in the ablation flux. One of them (the plume) contains the plasma of evaporated target material, which moves with the sound velocity corresponding to the plasma temperature. Another component is the relatively slow flow of droplets and debris ejected from the target surface by the shock wave, which is produced by the pressure pulse of laser-evaporated material. In this case, the velocity amounts to $\sim 2\times10^6$ cm s^{-1} at the maximum of the $V_e(\Phi_L)$ dependence, which corresponds approximately to the expansion velocity of the plasma plume estimated by scaling formulas given, for instance, in Refs [7, 38].

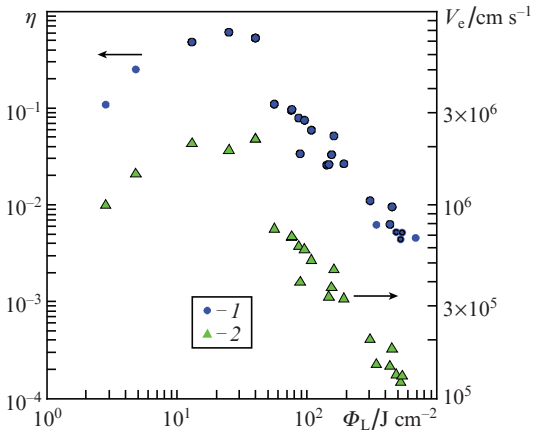

Figure 5. (Colour online) Dependences of (*1*) the ablation efficiency and (*2*) average velocity of the ablation flow on the laser energy density in the irradiation of a chondrite target of density $\chi = 27$ MPa.

With increasing energy density, the main part of the energy of laser pulses continues to go to plasma heating, with the result that the plasma expansion velocity becomes higher and only a small fraction of the energy is transferred to the target substance and is expended for the evaporation, melting, and fragmentation of the target. As Φ_L increases, the amplitude of the shock wave nevertheless becomes higher and the droplets and debris account for a progressively increasing fraction of removed mass, although the disruption efficiency remains low. In this case, if it is assumed that the laser pulse energy is entirely expended for increasing the kinetic energy of plasma plume expansion, it is easy to estimate that the mass carried away by the ablation stream turns out to be significantly smaller than the experimentally recorded mass. Therefore, although the bulk of energy goes to heat the plasma, its high expansion rate corresponds to the small mass contained in the plasma of the plume and gives a low average velocity and a low efficiency on averaging. Note that in the simulations of crater size in Refs [25, 39] the energy expenditures for surface disruption were calculated from precisely the specific melting energy of the target material.

In this connection it is believed that the significant difference of the scalings for mass removal ($\mu \propto \Phi_L^{1.2}$) and impulse coupling coefficient ($C_m \propto \Phi_L^{-0.66}$) measured in our work from the corresponding scalings for metals known from the literature is due to the lower strength and lower plasticity of polycrystalline stone targets.

4. Conclusions

As a result of our research, the ablation characteristics of stone polycrystalline targets of complex multicomponent composition (artificial chondrite targets and targets made of natural andesite) were determined, as far as we know, for the first time. The case in point is the mass removal, the specific disruption energy, the impulse coupling coefficient, the average velocity of ablation flow, and the ablation efficiency. The targets were irradiated by the neodymium laser pulses of nanosecond duration at an energy density of up to 5×10^4 J cm^{-2}. We showed that, although the absolute values of ablation parameters were close to those measured for metals, the forms of the dependences were significantly different. Our experiments demonstrated the existence of two ablation regimes, the boundary between which lies in the region $\Phi_L \approx 4000$ J cm^{-2}. The regime change is characterised by the variation of the form the dependence of mass removal μ on the laser energy density and the appearance of a minimum in the dependence of the specific disruption on Φ_L. It is believed that the change of ablation characteristics on exceeding the boundary Φ_L value is related to the passage from the one-dimensional expansion of the plasma plume to the three-dimensional one and therefore to a lowering of the efficiency of energy transfer from the laser pulse to the target owing to a density lowering of the laser-produced plasma.

Our experiments have also shown the existence of a maximum in the dependence of impulse coupling coefficient on the laser energy density ($C_m \approx 6.3\times10^{-5}$ N W^{-1} for $\Phi_L = \Phi_{opt} \approx 25$ J cm^{-2}). Maxima were also recorded in the Φ_L dependences of the ablation efficiency and the average velocity of ablation flow. We note that the maximum of C_m for metals and polymer materials is reached for Φ_L values that are several times lower than those measured for stone targets in our work. Furthermore, in the laser energy density domain $\Phi_L > \Phi_{opt}$, approximating the resultant data shows that $C_m \propto \Phi_L^{-n}$ with the exponent $n = 0.66$, unlike metals and polymer materials characterised by a significantly gentler sloping ($n \approx 0.3$) decay of $C_m(\Phi_L)$, which is confirmed by the experiments on the iron-nickel target carried out in the present work. This difference is supposedly due to the lower strength and lower plasticity of the polycrystalline stone targets.

In the analysis of the resultant data it is well to bear in mind that our experiments were carried out for relatively small dimensions of irradiation spot comparable with the characteristic size of the structural inhomogeneity of real polycrystalline rock formation. At the same time, as shown by experiments, the data scatter for the most inhomogeneous samples (natural andesite) did not exceed 10% – 20% irrespective of irradiation point. Of course, however, to eliminate the factor of target composition inhomogeneity, in the future it will be necessary to perform experiments for samples of larger size with an irradiation spot size (~1 cm) much greater than the characteristic size of main inhomogeneities of polycrystalline mountain rock with the use of laser beams of significantly greater energy.

We emphasise that our resultant data may be used in the optimisation of laser irradiation parameters in laser ablation as the source of jet thrust for deflecting natural cosmic objects from their orbits that pass in the dangerous vicinity of the Earth.

Acknowledgements. The authors consider it their pleasant duty to thank E.Yu. Aristova, S.G. Garanin, V.N. Dergach, V.G. Rogachev, and P.V. Starodubtsev, the staff members of the Institute of Laser Physics Research, Russian Federal Nuclear Centre–All-Russian Scientific Research Institute of Experimental Physics, for their constant interest in the work, for providing artificial chondrite targets and useful discussions of the results. We express our appreciation to A.P. Kuznetsov, K.L. Gubskii, and M.A. Gorbasheva, the staff members of the National Nuclear Research University MEPhI, for placing a PDV metre at our disposal and for their assistance in measuring the impulse coupling coefficient.

References

1. Shustov B.M., Rykhlova L.V. *Asteroidno-kometnaya opasnost': vchera, segodnya, zavtra* (Asteroid-Comet Hazard: Yesterday, Today, Tomorrow) (Moscow: Fizmatlit, 2013).
2. Phipps C. *AIP Conf. Proc*., **1278**, 502 (2010).
3. Thiry N., Vasile M. *Acta Astronautica*, **140**, 293 (2017).
4. Phipps C.R., Boustie M., et al. *J. Appl. Phys*., **122**, 193103 (2017).
5. Phipps C.R., Dreyfus R.W., in *Laser Microprobe Analysis* (New York: John Wiley, 1993) p. 369.
6. Kelly R., Dreyfus R.W. *Nucl. Inst. Meth. B*, **32**, 341 (1988).
7. Phipps C.R., Turner T.P., et al. *J. Appl. Phys*., **64**, 1083 (1988).
8. Phipps C.R., Birkan M., Bohn W., et al. *J. Propulsion Power*, **26**, 609 (2010).
9. Phipps C.R., Bonnal C., et al. *Acta Astronautica*, **146**, 92 (2018).
10. Rezunkov Yu.A. *Izv. Vyssh. Uchebn. Zaved., Ser. Priborostroenie*, **54**, 7 (2011).
11. Vasile M., Maddock C. *Adv. Space Res*., **50**, 891 (2012).
12. Loktionov E.Yu., Protasov Yu.S., Protasov Yu.Yu. *Opt. Spektrosk.*, **115**, 849 (2013).
13. Burdonskii I.N., Gol'tsov A.Yu., Leonov A.G., et al. *Vopr. Atom. Nauki i Tekhn., Ser. Termoyad. Sintez*, **36**, 8 (2013).
14. Timofeev I.S., Aleksandrov N.L., et al. *Laser Phys*., **24**, 12 (2014).
15. Day J.M.D., Ash R.D., Liu Y., et al. *Nature*, **457**, 179 (2009).
16. Rieder R., Economou T., Waeenke H., et al. *Science*, **278**, 1771 (1997).
17. http://geo.web.ru/db/meteorites/card.html?id=10572.
18. Aristova E.Yu., Aushev A.A., Baranov V.K., et al. *J. Exp. Theor. Phys*., **126**, 132 (2018) [*Zh. Eksp. Teor. Fiz*., **153**, 157 (2018)].
19. Kozlovskii E.A. (Ed.) *Gornaya entsiklopediya* (Mountain Encyclopaedia) (Moscow: Sov. Entsiklopediya, 1984–1991).
20. Gorbashova M., Burdonskiy I., Gubskiy K., et al. *J. Phys: Conf. Ser*., **941**, 012002 (2017).
21. Gorbasheva M.A., Gubskii K.L., Yufa V.N., et al. *Trudy Konf. 'LaPlaz-2018'* (Proc. IV Int. Conf. on Laser and Plasma Research and Technologies 'LaPlaz 2018') (Moscow: NIYaU MIFI, 2018) p. 463.
22. Mulser P., Bauer D. *High Power Laser-Matter Interaction* (Berlin– Heidelberg: Springer, 2010).
23. Stafe M., Marcu A., Puscas N.N. *Pulsed Laser Ablation of Solids. Basics, Theory and Applications* (Berlin–Heidelberg: Springer-Verlag, 2014, Springer Series in Surface Sciences) Vol. 53.
24. Anisimov S.I., Imas Ya.A., Romanov G.S., Khodyko Yu.V. *Deistvie izlucheniya bol'shoi moshchnosti na metally* (Action of High-Power Radiation on Metals) (Moscow: Nauka, 1970).
25. Gus'kov K.S., Gus'kov S.Yu. *Quantum Electron*., **31**, 305 (2001) [*Kvantovaya Elektron*., **31**, 305 (2001)].
26. Anisimov S.I., Luk'yanchuk B.S. *Phys. Usp*., **45**, 293 (2002) [*Usp. Fiz. Nauk*, **172**, 301 (2002)].
27. Hoffman J., Chrzanowska J., et al. *Appl. Phys. A*, **117**, 395 (2014).
28. Sucharita S. *J. Laser Appl*., **30**, 012008 (2018).
29. Gus'kov S.Yu., Borodzyuk S., Kalal M., et al. *Quantum Electron*., **34**, 989 (2004) [*Kvantovaya Elektron*., **34**, 989 (2004)].
30. Margarone D., Láska L., et al. *Appl. Surf. Sci*., **254**, 2797 (2008).
31. Gurvich L.V., Veits I.V., Medvedev V.A., et al. *Termodinamicheskie svoistva individual'nykh veshchestv* (Thermodynamic Properties of Individual Substances) (Moscow: Nauka, 1979) Vol. II, book 1.
32. Zuiani F., Vasile M., Gibbings A. *Celest. Mech. Dyn. Astron*., **114**, 107 (2012).
33. *Fizicheskie svoistva gornykh porod i poleznykh iskopaemykh (petrofizika). Spravochnik geofizika* [Physical Properties of Mountain Rock and Minerals (Petrophysics). Handbook of Geophysicists] (Moscow: Izd. 'Nedra', 1984).
34. Belov M.A., Cherepetskaya E.B. *Obozr. Prikl. Prom. Mat*., **10**, 756 (2004).
35. Grun J., Obenschain S.P., Ripin B.H., et al. *Phys. Fluids*, **26**, 588 (1983).
36. Gregg D.W., Thomas S.J. *J. Appl. Phys*., **37**, 2787 (1966).
37. Bonch-Bruevich A.M., Imas Ya.A. *Zh. Tekh. Fiz*., **37**, 1917 (1967).
38. Mora P. *Phys. Fluids*, **25**, 1051 (1982).
39. Gus'kov S.Yu., Kasperchik A., Pisarchik T., et al. *J. Exp. Theor. Phys.*, **105**, 793 (2007) [*Zh. Eksp. Teor. Fiz*., **132**, 907 (2007)].